Magnetoelastic effects in $Ni_2Mn_{1+x}Ga_{1-x}$ alloys from first-principles calculations

Qing-Miao Hu,[1,2,*] Chun-Mei Li,[1,2] Svetlana E. Kulkova,[3] Rui Yang,[1] Börje Johansson,[2,4,5] and Levente Vitos[2,4,6]
[1]*Shenyang National Laboratory for Materials Science, Institute of Metal Research, Chinese Academy of Sciences, 72 Wenhua Road, Shenyang 110016, China*
[2]*Applied Materials Physics, Department of Materials Science and Engineering, Royal Institute of Technology, Stockholm SE-100 44, Sweden*
[3]*Institute of Strength Physics and Materials Science, Siberian Branch of Russian Academy of Science, 2/4 Akademichesky, Tomsk 634021, Russia*
[4]*Condensed Matter Theory Group, Physics Department, Uppsala University, Uppsala SE-75121, Sweden*
[5]*School of Physics and Optoelectronic Technology, College of Advanced Science and Technology, Dalian University of Technology, Dalian 116024, China*
[6]*Research Institute for Solid State Physics and Optics, P.O. Box 49, Budapest H-1525, Hungary*
(Received 11 September 2009; revised manuscript received 3 November 2009; published 16 February 2010)

The magnetic coupling between Mn atoms on Ga sublattice (Mn_{Ga}) and Mn atoms on Mn sublattice (Mn_{Mn}) in $Ni_2Mn_{1+x}Ga_{1-x}$ alloy and its effect on the elastic modulus of the alloy are investigated by the use of first-principles methods. It is shown that, for $x=0.25$, the state with antiparallel Mn_{Ga}-Mn_{Mn} magnetic coupling is slightly more stable than that with parallel coupling, whereas for $x=0.10$, both magnetic states are almost degenerated. For both antiparallel and parallel Mn_{Ga}-Mn_{Mn} magnetic couplings, the bulk modulus (B) of $Ni_2Mn_{1+x}Ga_{1-x}$ deviates from the general e/a-B relationship with e/a being the number of valence electrons per atom. The shear modulus C' versus the martensitic transformation temperature T_M for $Ni_2Mn_{1+x}Ga_{1-x}$ with antiparallel Mn_{Ga}-Mn_{Mn} magnetic coupling is in line with the general C'-T_M relationship for Ni_2MnGa-based alloys, in contrast to the case of parallel Mn_{Ga}-Mn_{Mn} magnetic coupling.

DOI: 10.1103/PhysRevB.81.064108 PACS number(s): 31.15.es, 75.50.Cc, 62.20.fg, 64.70.kd

The ferromagnetic Ni_2MnGa-based alloys have drawn much attention in recent years due to their attractive properties such as magnetic field induced shape memory effect (e.g., Refs. 1 and 2) and large magnetocaloric effect (e.g., Refs. 3 and 4), resulting from the coupling between the magnetic and structural phase transitions. Alloys showing such properties generally possess compositions off the standard stoichiometry. Because of that, investigations of the magnetic states of the off-stoichiometric Ni_2MnGa are crucial for understanding their properties. First-principles methods are ideal theoretical tools for such purposes and have been widely used to study the crystallographic and magnetic structure of the Ni_2MnGa-based alloys.[5–12] However, the first-principles investigation of the magnetic coupling between the atoms in off-stoichiometric Ni_2MnGa alloys (especially those with excess Mn atoms, Mn being the main source of the magnetism in these alloys) and its effect on the properties have rarely been found in literature due to the complexity of the problem.

Previously (Ref. 13) we investigated the site occupancy, magnetic moments, and elastic modulus of nine types of off-stoichiometric Ni_2MnGa alloys using the first-principles exact muffin-tin orbital (EMTO) method[14,15] in combination with coherent-potential approximation (CPA).[16–18] We demonstrated that, for the Mn-rich and Ga-deficient Ni_2MnGa-based alloy, the excess Mn atoms prefer to occupy the Ga sublattice. Depending on the compositions of the alloys, magnetic moment of Mn antisite on Ga sublattice (denoted as Mn_{Ga}) can be parallel (for $Ni_2Mn_{1+x}Ga_{1-x}$) or antiparallel (for $Ni_{2-2x}Mn_{1+3x}Ga_{1-x}$) to those of the Mn atoms on Mn sublattice (denoted as Mn_{Mn}). Hereafter, the parallel and antiparallel Mn_{Ga}-Mn_{Mn} magnetic couplings are denoted as P and AP states, respectively. The calculation of the elastic modulus shows that the bulk moduli (B) of these types of alloys are not in line with the general e/a-B relationship (e/a ratio being the number of valence electrons per atom) for the off-stoichiometric Ni_2MnGa alloys, i.e., a larger e/a ratio corresponds to a harder B.[13] It was suggested that this feature might be due to the magnetic interaction between Mn_{Ga} and Mn_{Mn} since the bulk moduli from paramagnetic calculations follows the general e/a-B relationship. Furthermore, the shear modulus C' of $Ni_2Mn_{1+x}Ga_{1-x}$ with parallel Mn_{Ga}-Mn_{Mn} magnetic coupling is found to be an exception of the general C'-T_M trend, i.e., a softer C' indicates a higher T_M. These results inspired us to carry out a more detailed investigation on the magnetic coupling between Mn_{Ga} and Mn_{Mn} and its effect on the elastic modulus of the alloys with excess Mn atoms.

In this paper, $Ni_2Mn_{1+x}Ga_{1-x}$ alloy was selected to study the magnetic coupling between Mn_{Ga} and Mn_{Mn} by the use of the first-principles methods based on density-functional theory.[19] The Mn_{Ga}-Mn_{Mn} magnetic coupling in this alloy has be investigated with regard to different c/a of the tetragonal phase by Enkovaara *et al.*[23] Here, we focus on the equation of states and elastic moduli of the high-temperature $L2_1$ phase with both P and AP magnetic states.

We first calculated the equation of states of $Ni_2Mn_{1+x}Ga_{1-x}$ using both full-potential augmented plane-wave (FPAPW) (Ref. 20) and EMTO (Refs. 14 and 15) methods with the supercell geometry. One of the four Ga atoms in the $L2_1$ crystallographic cell was replaced by an Mn atom, corresponding to $x=0.25$. WIEN2K package[21] was employed for the FPAPW calculations, where the muffin-tin radii for Ni, Mn, and Ga were set as 2.2, 2.2, and 2.1 a.u., respectively, and the plane-wave cutoff is 16 Ry. For the EMTO calculations, we chose the calculation parameters ex-

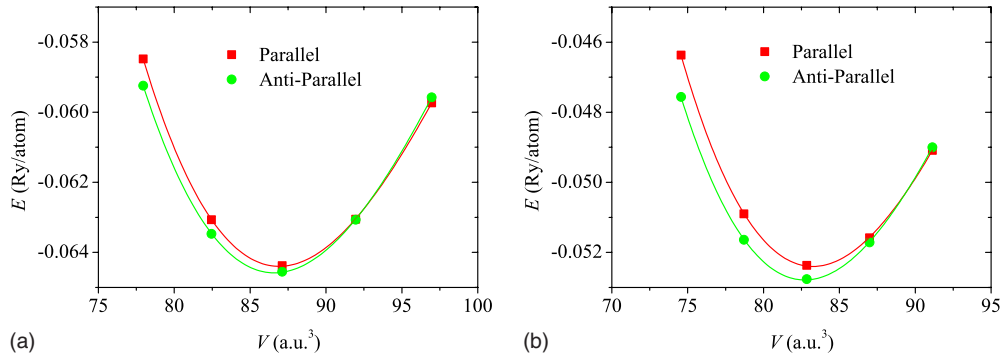

FIG. 1. (Color online) Equation of states of $Ni_2Mn_{1+x}Ga_{1-x}$ (x=0.25). (a) and (b) for the energy versus volume from EMTO and FPAPW calculations, respectively.

actly the same as those detailed in Ref. 13 in order to make the present results comparable to those reported in the reference. For both methods, the equation of states were obtained without relaxing the internal atomic positions. Our FPAPW test calculations show that the influence of the relaxation of the atomic positions on the equation of state is negligible. The calculations were performed with k-point mesh of 6 $\times 6 \times 6$ for the Brillouin zone sampling and general gradient approximation parameterized by Perdew, Burke, and Ernzerhof[22] for the electronic exchange-correlation functional.

For both FPAPW and EMTO methods, it is noted that, if started with parallel/antiparallel Mn_{Ga}-Mn_{Mn} magnetic coupling, the spin-polarized self-consistent calculations converge to the solutions without changing the initial magnetic orientation. Figures 1(a) and 1(b) show the curves of the total energy E versus volume V from both EMTO and FPAPW calculations. It is seen that both methods yield similar equation of states. Around equilibrium volume and smaller, the AP state is slightly more stable than the P state. The latter becomes more stable only if the volume is expanded. The enthalpy with respect to pressure was also calculated. Comparing the enthalpies of the P and AP states, we obtain that the AP to P transition occurs at pressure of about −10 GPa from FPAPW calculations and slightly larger from EMTO calculations.

Listed in Table I are the equilibrium properties of $Ni_2Mn_{1+x}Ga_{1-x}$ (x=0.25). The lattice constants from FPAPW calculations are smaller than those from EMTO and vice versa for the bulk modulus, which is due to the relatively small basis set and frozen-core approximation adopted in the EMTO calculations as discussed in Ref. 13. For both first-principles methods, the lattice constant of the alloy with AP state is larger than that with P state, whereas the bulk modulus for the AP state is slightly smaller than that for the P state. This, to some extent, might be related to the change in the magnetic moment of Ni atoms from P to AP state. As shown in Table I, the magnetic moment of Ni atom decreases from the P to AP state, whereas those of Mn and Ga atoms do not change significantly except that the magnetic moment of the Mn_{Ga} atom alters its orientation. Figure 2 shows the density of states of Ni atoms for both P and AP states from FPAPW calculations. It is seen that, in the minority DOS for P state, there exists a pseudogap at the energy around −1.5 eV, which is mainly resulted from the hybridization between the electronic states of Ni and Ga atoms.[10] For the AP state, an additional state occurs at about −0.7 eV in the pseudogap of the minority DOS, which is responsible for the decrease in the magnetic moment of Ni atoms from P to AP state. This additional state represents the weakening of the hybridization between the states of Ni and Ga from P and AP state, and therefore, might result in the increasing lattice constant and decreasing bulk modulus accordingly.

The AP state is a fraction of millirydberg per atom more

TABLE I. Properties of $Ni_2Mn_{1+x}Ga_{1-x}$ alloys with parallel and antiparallel magnetic couplings between Mn atoms on the Ga sublattice (Mn_{Ga}) and Mn on the Mn sublattice (Mn_{Mn}). a_0 is the equilibrium lattice constants in angstrom. $\Delta E = E^{AP} - E^{P}$, where E^{AP} and E^{P} are the energies (in mRy/atom) of the alloys with antiparallel and parallel Mn_{Ga} and Mn_{Mn} magnetic couplings, respectively. μ_0, μ_X (X=Ni, Mn, and Ga), and μ'_{Mn} (for Mn_{Ga}) are the total and local magnetic moments (in μ_B). B_0, C', C_{44} are the bulk and shear muduli (in GPa). e/a is the number of valence electrons per atom.

Method	System	a_0	ΔE	μ_0	μ_{Ni}	μ_{Mn}	μ_{Ga}	μ'_{Mn}	B_0	C'	C_{44}	e/a
FPAPW (SC)	x=0.25(P)	5.8229	0	5.33	0.50	3.38/3.42	−0.03	3.52	156.1			−7.75
	x=0.25(AP)	5.8099	−0.38	3.12	0.32	3.32/3.42	−0.03	−3.45	156.0			−7.75
EMTO (SC)	x=0.25(P)	5.9073	0	5.21	0.38	3.56/3.62	−0.08	3.68	148.5			−7.75
	x=0.25(AP)	5.9001	−0.19	3.06	0.23	3.54/3.62	−0.07	−3.70	147.7			−7.75
EMTO-CPA	x=0.10(P)	5.8977	0	4.51	0.33	3.56	−0.03	3.20	148.6	16.0	99.6	7.60
	x=0.10(AP)	5.8948	~0	3.65	0.27	3.54	−0.11	−3.26	147.9	13.5	100.6	7.60
EMTO	x=0.00	5.8922		4.27	0.29	3.54	−0.07		151.9	15.9	99.4	7.50

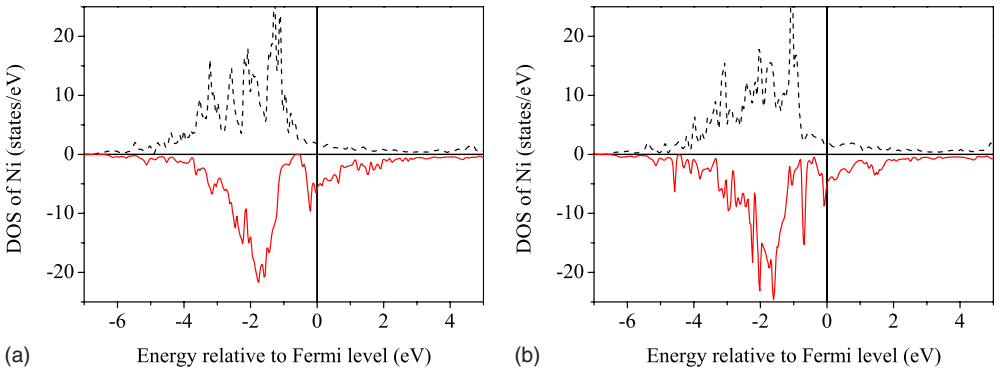

FIG. 2. (Color online) Density of states of Ni atom in $Ni_2Mn_{1+x}Ga_{1-x}$ (x=0.25) for both (a) parallel and (b) antiparallel Mn_{Ga}-Mn_{Mn} magnetic couplings from FPAPW calculations.

stable than the P state. Since $Ni_2Mn_{1+x}Ga_{1-x}$ alloy prefers the AP state to the P state, the ferromagnetic Ni_2MnGa will gradually transform to antiferromagnetic state with increasing concentration of excess Mn, so that the saturation magnetization of the alloy decreases accordingly, which is in agreement with the experiments of Enkovaara *et al.*[23] and Albertini *et al.*[24] The more stable AP state of $Ni_2Mn_{1+x}Ga_{1-x}$ (x=0.25) has also been found theoretically by Enkovaara *et al.*[23] using full-potential linearized augmented plane-wave method.

In Ref. 13, we reported that $Ni_2Mn_{1+x}Ga_{1-x}$ (x=0.10) shows anomalous bulk modulus B and shear modulus C' compared to the general e/a-B and C'-T_M relationships for off-stoichiometric Ni_2MnGa alloys. It is interesting to know whether this abnormal elastic modulus stems from the Mn_{Ga}-Mn_{Mn} magnetic coupling or not. In this regard, we investigated the Mn_{Ga}-Mn_{Mn} magnetic coupling in $Ni_2Mn_{1+x}Ga_{1-x}$ (x=0.10) using the EMTO method. Since $Ni_2Mn_{1+x}Ga_{1-x}$ (x=0.10) is inconvenient to be described as a supercell, the CPA was adopted to described the system, assuming that the excess Mn atoms distributed randomly on the Ga sublattice.

Figure 3 shows the curves of total energy versus volume of the alloy with both P and AP states of $Ni_2Mn_{1+x}Ga_{1-x}$ (x=0.10). Similar to the high-concentration (x=0.25) case, the AP state is slightly more stable than the P state when the system is compressed whereas the latter is more stable when the system is expanded. However, the energy difference between both states is much smaller compared to the high-concentration off-stoichiometric alloys. At the equilibrium state, the P and AP states are almost degenerated with an energy difference close to the accuracy of the employed first-principles method. The vanishing energy difference between the P and AP states may be ascribed to three facts. (1) With fixed number of Mn_{Ga} (and therefore, fixed local magnetic interaction difference between the P and AP states) and increasing total number of atoms in the system, i.e., decreasing concentration of Mn_{Ga}, the total energy difference per atom is expected to decrease. (2) Compared to the case of the high Mn_{Ga} concentration, the magnetic interaction between Mn_{Ga} atoms is largely absent in the case of low Mn_{Ga} concentration, which further decreases the total-energy difference. (3) As shown by the supercell calculations with x=0.25, EMTO calculations with muffin-tin potential underestimates the total-energy difference compared to the FPAPW calculations. Therefore, although the energy difference per atom between the P and AP configurations vanishes at low Mn_{Ga} concentration, the AP could be still more stable if observing locally around Mn_{Ga}. Comparing to the EMTO supercell cell calculations with x=0.25, the magnetic moments of the Mn atoms on the Mn sublattice, Ni and Ga atoms do not change significantly, but that of the Mn_{Ga} decreases.

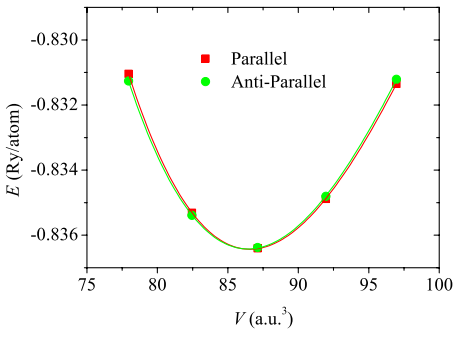

FIG. 3. (Color online) Total energy versus volume of the $Ni_2Mn_{1+x}Ga_{1-x}$ (x=0.10) alloy with parallel and antiparallel Mn_{Ga}-Mn_{Mn} magnetic couplings.

With the antiparallel Mn_{Ga}-Mn_{Mn} magnetic coupling, we calculated the shear moduli C' and C_{44} as well as the bulk modulus B of $Ni_2Mn_{1+x}Ga_{1-x}$ (x=0.10). Details of the calculations of the elastic modulus can be found in Ref. 13. We obtained C' of 13.5 GPa, C_{44} of 100.6 GPa, and B of 147.9 GPa for the AP state, in comparison with 16.0, 99.6, and 148.6 GPa for the P state as listed in Table I. The elastic moduli of $Ni_2Mn_{1+x}Ga_{1-x}$ (x=0.10) versus e/a ratio are plotted in Fig. 4 together with those of the nine types of off-stoichiometric Ni_2MnGa-based alloys reported in Ref. 13. As shown in Fig. 4, the bulk modulus of $Ni_2Mn_{1+x}Ga_{1-x}$ (x=0.10) with AP state is still smaller than that of the ideal Ni_2MnGa, deviating significantly from the general e/a-B relationship. The data points of the shear moduli, C_{44} and C', versus e/a for $Ni_2Mn_{1+x}Ga_{1-x}$ (x=0.10) with AP state are getting closer to the fitting curves, matching better to the general C_{44}-e/a and C'-e/a relationships than those with P state.

The C' (16.0 GPa) of $Ni_2Mn_{1+x}Ga_{1-x}$ (x=0.10) with P state is at the same level as that of the perfect Ni_2MnGa

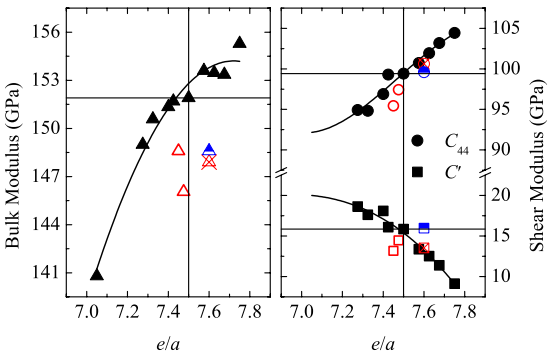

FIG. 4. (Color online) Bulk (left panel) and shear (right panel) moduli of off-stoichiometric Ni_2MnGa alloys with respect to e/a ratio. The vertical and horizontal lines within the figures refer to the elastic moduli and e/a ratio of the standard stoichiometric Ni_2MnGa. The crossed symbols refer to the data point of the $Ni_2Mn_{1+x}Ga_{1-x}$ (x=0.10) alloy with antiparallel Mn_{Ga}-Mn_{Mn} magnetic coupling and the half-filled symbols for those with parallel Mn_{Ga}-Mn_{Mn} magnetic coupling. The solid triangles, circles, and squares represent, respectively, the bulk moduli, C_{44}, and C' of the nine kinds of off-stoichiometric Ni_2MnGa alloys, taken from Ref. 13, in which the open ones are for the Mn-rich and Ga-deficient alloys of which the bulk moduli deviate the general e/a-B relationship. The fitting curves are to guide the view.

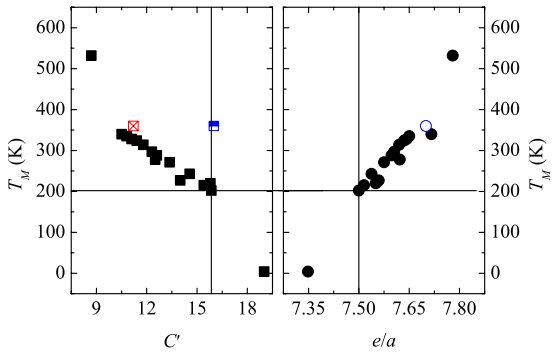

FIG. 5. (Color online) Experimental martensitic transformation temperature (T_M) with respect to the shear modulus C' (left panel) and e/a ratio (right panel) of the off-stoichiometric Ni_2MnGa alloys. The vertical lines within the figures refer to the C' and e/a ratio and the horizontal lines refer to the T_M of the standard stoichiometric Ni_2MnGa. The crossed symbol refers to the data point of the $Ni_2Mn_{1+x}Ga_{1-x}$ (x=0.10) alloy with antiparallel Mn_{Ga}-Mn_{Mn} magnetic coupling and the half-filled symbol to that with parallel Mn_{Ga}-Mn_{Mn} magnetic coupling, whereas the others are taken from Ref. 13.

(15.9 GPa), indicating that their martensitic transformation temperatures T_M should also be close to each other according to the general C'-T_M trend as discussed in Ref. 13. However, experiments have shown that T_M of $Ni_2Mn_{1+x}Ga_{1-x}$ increases with x. As an example, the measured T_M of $Ni_2Mn_{1+x}Ga_{1-x}$ (x=0.20) is about 360 K,[24] in comparison with T_M=202 K for ideal Ni_2MnGa.[25] On the other hand, with the AP state, the calculated C' of $Ni_2Mn_{1+x}Ga_{1-x}$ (x=0.10) is smaller than that of the perfect Ni_2MnGa, corresponding to a higher T_M of $Ni_2Mn_{1+x}Ga_{1-x}$ than that of Ni_2MnGa, in line with the general C'-T_M trend. The C' of $Ni_2Mn_{1+x}Ga_{1-x}$ (x=0.20) with AP state is evaluated to be 11.2 GPa by a linear extrapolation of the C'-x relationship determined by the C' of $Ni_2Mn_{1+x}Ga_{1-x}$ (x=0.10) and that of the ideal Ni_2MnGa. In Fig. 5, we plotted the T_M versus C' of $Ni_2Mn_{1+x}Ga_{1-x}$ (x=0.20) together with those reported in Ref. 13. It is seen that the T_M versus C' of $Ni_2Mn_{1+x}Ga_{1-x}$ (x=0.20) with AP state fits the general C'-T_M trend very well. In this sense, both e/a ratio and C' can be considered as qualitative predictors of the composition-dependent T_M of Ni_2MnGa-based alloy.

In summary, we have investigated the magnetic coupling between Mn atoms on Ga sublattice (Mn_{Ga}) and Mn atoms on Mn sublattice (Mn_{Mn}) in $Ni_2Mn_{1+x}Ga_{1-x}$ alloys using first-principles methods. It was shown that, for x=0.25, the state with antiparallel Mn_{Ga}-Mn_{Mn} magnetic coupling is slightly more stable than that with parallel coupling, whereas for x=0.10, they are almost degenerated. The bulk modulus of $Ni_2Mn_{1+x}Ga_{1-x}$, no matter with antiparallel or parallel Mn_{Ga}-Mn_{Mn} magnetic coupling, deviates from the general e/a-B relationship. The shear modulus C' of the alloy changes significantly with parallel and antiparallel Mn_{Ga}-Mn_{Mn} magnetic couplings. For the antiparallel Mn_{Ga}-Mn_{Mn} magnetic coupling, the shear modulus C' versus the martensitic transformation temperature T_M is in line with the general C'-T_M relationship for Ni_2MnGa-based alloys, in contrast to the case for the parallel Mn_{Ga}-Mn_{Mn} magnetic coupling.

The authors acknowledge the financial support from the MoST of China under Grant No. 2006CB605104, from the NSFC under Grants No. 50871114 and No. 08-02-92201a (RFBR-NSFC project for the Sino-Russian cooperation). The Swedish Research Council, the Swedish Foundation for Strategic Research, the Hungarian Scientific Research Fund (Grant No. T048827), and the Carl Tryggers Foundation are also acknowledged for financial support.

*Corresponding author; qmhu@imr.ac.cn

[1] A. Sozinov, A. A. Likhachev, N. Lanska, and K. Ullakko, Appl. Phys. Lett. **80**, 1746 (2002).

[2] K. Oikawa, T. Ota, Y. Tanaka, H. Morito, A. Fujita, R. Kainuma, K. Fukamichi, and K. Ishia, Appl. Phys. Lett. **81**, 5201 (2002).

[3] F. X. Hu, B. G. Shen, J. R. Sun, and G. H. Wu, Phys. Rev. B **64**, 132412 (2001).

[4] J. Marcos, A. Planes, L. Manosa, F. Casanova, X. Batlle, A. Labarta, and B. Martinez, Phys. Rev. B **66**, 224413 (2002).

[5] A. Ayuela, J. Enkovaara, K. Ullakko, and R. M. Nieminen, J. Phys.: Condens. Matter **11**, 2017 (1999).

[6] S. Fujii, S. Ishida, and S. J. Asano, J. Phys. Soc. Jpn. **58**, 3657 (1989).

[7] J. Kübler, A. R. Williams, and C. B. Sommers, Phys. Rev. B **28**,

1745 (1983).
[8] A. T. Zayak, P. Entel, J. Enkovaara, A. Ayuela, and R. M. Nieminen, J. Phys.: Condens. Matter **15**, 159 (2003); Phys. Rev. B **68**, 132402 (2003).
[9] Claudia Bungaro, K. M. Rabe, and A. Dal Corso, Phys. Rev. B **68**, 134104 (2003).
[10] S. R. Barman, S. Banik, and Aparna Chakrabarti, Phys. Rev. B **72**, 184410 (2005).
[11] Jie Chen, Yan Li, Jiaxiang Shang, and Huibin Xu, Appl. Phys. Lett. **89**, 231921 (2006).
[12] P. Entel, M. E. Gruner, W. A. Adeagbo, C. J. Eklund, A. T. Zayak, H. Akai, and M. Acet, J. Magn. Magn. Mater. **310**, 2761 (2007).
[13] Q.-M. Hu, C.-M. Li, R. Yang, S. E. Kulkova, D. I. Bazhanov, B. Johansson, and L. Vitos, Phys. Rev. B **79**, 144112 (2009).
[14] L. Vitos, Phys. Rev. B **64**, 014107 (2001).
[15] L. Vitos, *Computational Quantum Mechanics for Materials Engineers* (Springer-Verlag, London, 2007).
[16] P. Soven, Phys. Rev. **156**, 809 (1967).
[17] B. L. Gyorffy, Phys. Rev. B **5**, 2382 (1972).
[18] L. Vitos, I. A. Abrikosov, and B. Johansson, Phys. Rev. Lett. **87**, 156401 (2001).
[19] R. M. Dreizler and E. K. U. Gross, *Density Functional Theory* (Springer, Berlin, 1998).
[20] K. Schwarz, P. Blaha, and G. K. H. Madsen, Comput. Phys. Commun. **147**, 71 (2002).
[21] P. Blaha, Karlheinz Schwarz, Georg Madsen, Dieter Kvasnicka, and Joachim Luitz, *WIEN2k: An Augmented Plane Wave Plus Local Oribitals Program for Calculating Crystal Properties* (Vienna University of Technology, Vienna, 2002).
[22] J. P. Perdew, K. Burke, and M. Ernzerhof, Phys. Rev. Lett. **77**, 3865 (1996).
[23] J. Enkovaara, O. Heczko, A. Ayuela, and R. M. Nieminen, Phys. Rev. B **67**, 212405 (2003).
[24] F. Albertini, A. Paoluzi, L. Pareti, M. Solzi, L. Righi, E. Villa, S. Besseghini, and F. Passaretti, J. Appl. Phys. **100**, 023908 (2006).
[25] P. J. Webster, K. R. A. Ziebeck, S. L. Town, and M. S. Peak, Philos. Mag. B **49**, 295 (1984).